



Dating the Tethyan Ocean in the Western Alps with radiolarite pebbles from synorogenic Oligocene molasse basins (southeast France)

Fabrice Cordey, Pierre Tricart, Stéphane Guillot, Stéphane Schwartz

► To cite this version:

Fabrice Cordey, Pierre Tricart, Stéphane Guillot, Stéphane Schwartz. Dating the Tethyan Ocean in the Western Alps with radiolarite pebbles from synorogenic Oligocene molasse basins (southeast France). Swiss Journal of Geosciences, 2012, 105 (1), pp.39-48. 10.1007/s00015-012-0090-8 . hal-02178343

HAL Id: hal-02178343

<https://hal.science/hal-02178343>

Submitted on 30 Jun 2021

HAL is a multi-disciplinary open access archive for the deposit and dissemination of scientific research documents, whether they are published or not. The documents may come from teaching and research institutions in France or abroad, or from public or private research centers.

L'archive ouverte pluridisciplinaire **HAL**, est destinée au dépôt et à la diffusion de documents scientifiques de niveau recherche, publiés ou non, émanant des établissements d'enseignement et de recherche français ou étrangers, des laboratoires publics ou privés.

Dating the Tethyan ocean in the Western Alps with radiolarite pebbles from synorogenic Oligocene molasse basins (southeast France)

Running title: Radiolarite pebbles from Alpine Oligocene molasses

Fabrice Cordey^{1*}, Pierre Tricart², Stéphane Guillot², Stéphane Schwartz²

¹Département des Sciences de la Terre, CNRS UMR 5276 Laboratoire de Géologie de Lyon,
Université Lyon 1, 69622 Villeurbanne, France

²IsTerre, CNRS, Université de Grenoble I, 38041 Grenoble, cedex 9, France

*corresponding author: fabrice.cordey@univ-lyon1.fr

Keywords: Western Alps, radiolarite, Jurassic, molasse, Oligocene, subduction wedge.

25 **Abstract**

26

27 For the first time in the Western Alps, radiolarite pebbles collected from Tertiary foreland
28 molasse conglomerates are treated for microfossil extraction and dated. Among fourty pebbles
29 selected in the field, seven of them released diagnostic radiolarian assemblages ranging in age
30 from Late Bajocian-Early Callovian to Middle Oxfordian-Early Tithonian. These ages overlap
31 previous biochronological data obtained from *in situ* localities of the Schistes Lustrés Piemont
32 zone of the French-Italian Alps and triple the number of diagnostic radiolarite samples known
33 so far in this segment of the chain. The diagnostic pebbles are characterized by low grade
34 metamorphism, showing that some eroded thrust-sheets from the oldest parts of the ocean
35 escaped any tectonic burial during the Alpine convergence. Mixing of low and high-grade
36 radiolarites, mafics and ultramafics pebbles implies that a variety of ocean-derived units was
37 exposed. This tectonic scenario involves tight refolding and severe uplift of the Eocene
38 subduction wedge in the Early Oligocene.

39

40

41 **1. Introduction**

42

43 The European Alps straddle the plate boundary between Europe and Africa where divergence
44 dominated during most of Jurassic-Cretaceous times followed by convergence from the Late
45 Cretaceous onwards (e.g. Tricart 1984). As a major witness to plate divergence, ophiolites
46 derive from a small Tethyan ocean basin, the Alpine Tethys also named Liguria, Liguria-
47 Piemont or Piemont-Liguria (review in Bernoulli and Jenkyns 2009, Lagabrielle 2009,
48 Manatschal and Müntener 2009, de Graciansky et al. 2010). In the Western Alps,
49 dismembered ophiolites and associated deep-sea sediments compose most of the Piemont

50 zone (review in Schmid et al. 2004). They display subduction-related HP-LT metamorphic
51 imprint evolving from blueschist facies in the outer Piemont units to eclogite facies in the
52 inner ones (review in Bousquet et al. 2008). As an exception, the Chenaillet ophiolite (Fig. 1)
53 escaped this metamorphism, suggesting that it derived from an obducted slab of oceanic
54 lithosphere (Mével et al. 1978, Barfety et al. 1995 with references therein).

55

56 Reconstructing the paleogeography of this vanished ocean at successive steps from
57 opening to closure remains a major challenge among Alpine geologists. Two difficulties
58 remained for a long time: the rarity of radiometric ages from ophiolites and the missing fossil
59 record due to metamorphism and/or erosion of sedimentary covers. Fortunately, some of the
60 Western Alps units closely resemble the unmetamorphic ophiolite thrust sheets of the
61 Northern Apennines which suggest that Tethyan ocean spreading occurred during the Middle-
62 Late Jurassic and possibly the Early Cretaceous (e.g. Lemoine et al. 1970, de Graciansky et al.
63 2010). Most modern reconstructions for the Western Alpine ocean derive from Marcel
64 Lemoine's sketches of the early 1980's. They show the Alpine Tethys and the Central
65 Atlantic as twin oceans for their initial opening and spreading (e.g. Lemoine 1983). On the
66 Tethyan European paleomargin, the transgressive units and their fossil record exposed in the
67 Briançonnais domain document the breakup unconformity (Lemoine et al. 1986) and provide
68 a Middle Jurassic age (Late Bathonian) for the timing of initial opening of the nearby ocean
69 (Lemoine et al. 2000, Bill et al. 2001).

70

71 A significant improvement came with the successive discovery and dating of three
72 radiolarite supraophiolitic localities: (1) the Cascavelier Peak near Saint-Véran in Southern
73 Queyras (De Wever and Caby 1981, De Wever and Baumgartner 1995), (2) the Traversiera
74 massif near the French-Italian border in the upper Ubaye valley (Schaaf et al. 1985, De Wever

75 et al. 1987, De Wever et Baumgartner 1995), and (3) more recently the Rocher de la Perdrix
76 in the Montgenèvre massif, located structurally below the Chenaillet ophiolite s.s. (Cordey
77 and Bailly 2007). In these three sites (Fig. 1), radiolarian faunas are preserved in low-
78 temperature blueschist-bearing metacherts at the front of the Piemont “Schistes lustrés”
79 complex (Gidon et al. 1994; Tricart et al. 2003). These three fossil localities directly argue for
80 an ocean opening during a period straddling the Middle and Late Jurassic times (Cordey and
81 Bailly 2007).

82

83 In order to improve our knowledge of the Alpine ocean history, we explored the
84 potential of synorogenic conglomerates derived from the erosion of oceanic thrust sheets
85 building the Alpine wedge. Rüst (1885) was the first to describe Jurassic radiolarians from
86 chert pebbles of western Switzerland molasses, but microfossil chemical extractions were not
87 yet applied at the time. A more recent interest for syn- or postorogenic clastics was developed
88 in the North American Cordillera on the well-known “chert pebble conglomerates” associated
89 with Mesozoic ocean sutures and accreted terranes (Seiders and Blome 1984; Cordey 1992a,
90 1992b, 1998). In this Alpine study, our objectives were not only to find new dates related to
91 the Jurassic opening of Tethys but also to document ocean closure and subsequent mountain
92 building during Early Oligocene time.

93

94

95 **2. The Oligocene polygenic conglomerates in the foreland of the southern Western Alps**

96

97 Within the Paleogene molasses of the Western Alps external zone, our investigation focused
98 on the French Subalpine chains located to the south of the Pelvoux massif (Ford et al. 1999,
99 Ford and Lickorish 2004). In this region, Early Oligocene intra-orogenic basins (Fig. 2)

100 contain conglomerates known for their ocean-derived pebbles (Termier 1895 in Gubler 1958,
101 Boussac 1912) such as fragments of mafics and ultramafics rocks as well as radiolarian chert
102 (Ferry et al. 2005). In the field, these radiolarite pebbles are easily recognizable by their dark
103 red colour (Fig. 3). They represent the “exotic” pebbles *par excellence*, occupying a
104 privileged position in the Alpine literature as symbols of a “Penninic” signature, the Swiss
105 term to describe the internal Alpine zones. The Early Oligocene molasses are preserved
106 within small basins in the foreland of the Paleogene Alpine accretionary wedge (e.g. Sissingh
107 2001) and were fed by clastic sediments derived from the erosion of uplifting Briançonnais
108 and Piemont zones (Morag et al. 2008; Bernet and Tricart 2011). Initially, our main target was
109 the Barrême basin, a small and well-studied valley located to the east of Digne thrust (de
110 Graciansky 1972, Artoni and Meckel 1998, Evans and Elliott 1999). A second site was found
111 farther north in the “Petit Buëch” valley near Montmaur (Fig. 1) where tectonically pinched
112 molasses named “Nagelfluh” correspond to the southward extension of the Devoluy basin
113 (Gidon 1971, Meckel et al. 1996).

114

115

116 **3. Biostratigraphic results: faunal assemblages and ages**

117

118 Seven diagnostic chert pebbles were found in a series of fourty selected in the field. Each
119 pebble was processed individually using standard chert-etching techniques with hydrofluoric
120 acid. Pebble 7064-E1 was collected at “La Poste de Clumanc” conglomerates (Fig. 2) near the
121 northern end of the Barrême basin (e.g. Chauveau and Lemoine 1961). Six pebbles numbered
122 7057-3 to 7057-22 were sampled in the “Petit Buëch” valley (Gidon 1971).

123

124 Pebbles faunal contents and ages are presented in Table 1. Key radiolarian taxa are illustrated
125 in Fig. 4. We use the standard Tethyan radiolarian zonation of Baumgartner et al. (1995)
126 based on Unitary Associations (UAZ) as well as complementary data from O'Dogherty et al.
127 (2006). The “age of a pebble” refers here to the age of the source radiolarite bed, not the age
128 of formation or deposition of the pebble.

129

130 Biochronology and ages are based on the following radiolarian occurrences:

131 - 7057-3: the assemblage contains *Archeospongoprunum* cf. *imlayi* Pessagno,
132 *Orbiculiformella* sp., *Stichocapsa robusta* Matsuoka, and *Stichocapsa* sp.. The age is
133 provided by the occurrence of *S. robusta* Matsuoka known from UAZ 5 to UAZ 7
134 corresponding to the Late Bajocian-Early Callovian interval.

135 - 7057-8 comprises *Cinguloturris carpatica* Dumitrica, *Praeconocaryomma* sp., *Stichocapsa*
136 aff. *robusta* Matsuoka (Fig. 4, n° 18) and ?*Stichomitra* sp. (Fig. 4, n° 14). This assemblage is
137 assigned to biozones UAZ 7-11 of Late Bathonian-Early Callovian to Late Kimmeridgian-
138 Early Tithonian age.

139 - 7057-14 contains *Acaeniotyle diaphorogona* Foreman (Fig. 4, n° 26), *Archeodictyomitra*
140 *apiarum* (Rüst), *Archeodictyomitra* sp. (Fig. 4, n° 7), *Cinguloturris carpatica* Dumitrica (Fig.
141 4, n° 4), *Emiluvia ordinaria* Ozvoldova, *Mirifusus* sp. (Fig. 4, n° 3), *Parahsuum carpathicum*
142 Widz & De Wever (Fig. 4, n° 11), ?*Parvingula mashitaensis* Mizutani (Fig. 4, n° 10),
143 *Podbursa* cf. *spinosa* Ozvoldova (Fig. 4, n° 24), *Protunuma* sp. (Fig. 4, n° 13),
144 *Pseudoeucyrtis* sp. (Fig. 4, n° 1), *Zhamoidellum ovum* Dumitrica (Fig. 4, n° 17) and
145 *Zhamoidellum* sp. (Fig. 4, n° 19). This assemblage is attributed to biozones UAZ 9-11 of
146 Middle Oxfordian to Early Tithonian age.

147 - 7057-15 contains a peculiar association which is not reported in Baumgartner et al. (1995)
148 biozonation but is documented by O'Dogherty et al. (2006): *Yaocapsa* sp. (Fig. 4, n° 12),

149 *Cinguloturris carpatica* Dumitrica, *Zhamoidellum* cf. *argandi* O'Dogherty, Gorican &
150 Dumitrica (Fig. 4, n° 16) and *Zhamoidellum* cf. *calamin* O'Dogherty, Gorican & Dumitrica
151 (Fig. 4, n° 22). This assemblage is tentatively assigned to UAZ 6-7 (O'Dogherty et al. 2006).
152 - 7057-20 contains *Archeodictyomitra apiarum* (Rüst), *Bernoullius* cf. *dicera* Baumgartner
153 (Fig. 4, n° 29), *Praeconocaryomma* sp. and *Stichocapsa* sp.. It provides a Middle Callovian-
154 Early Kimmeridgian age (UAZ 8-10). As the occurrence of species *B. dicera* Baumgartner is
155 uncertain, the upper age limit of this association is tentative.
156 - 7057-22: correlation to biozone UAZ 7 of Late Bathonian-Early Callovian age is provided
157 by co-occurrence of *Cinguloturris carpatica* Dumitrica (Fig. 4, n° 4) and *Pseudoristola*
158 *tsunoensis* (Aita) (Fig. 4, n° 22). Other radiolarians compatible with this age determination are
159 *Williriedellum* sp. 1 (Fig. 4, n° 23) only documented in Les Gets nappe along with
160 morphotypes from UAZ 6 and 7 (O'Dogherty et al. 2006) and *Archeospongoprnum elegans*
161 Wu (Fig. 4, n° 2) also known in this time interval. Other morphotypes present in 7057-14 are
162 *Arcanicapsa* cf. *leiostraca* (Foreman) (Fig. 4, n° 21), *Archeodictyomitra* sp. (Fig. 4, n° 8),
163 *Cinguloturris* sp. (Fig. 4, n° 5), *Emiluvia* cf. *chica* Foreman (Fig. 4, n° 27), ?*Fultocapsa* sp.
164 (Fig. 4, n° 25), *Homoeoparonaella argolidensis* Baumgartner (Fig. 4, n° 28), *Mirifusus* sp.,
165 *Pseudodictyomitrella* cf. *tuscanica* Chiari, Cortese & Marcucci (Fig. 4, n° 15), and *Tritrabs*
166 *rhododactylus* Baumgartner (Fig. 4, n° 30).
167 - 7064-E1 contains *Archeodictyomitra apiarum* (Aita) (Fig. 4, n° 4), *Archeospongoprnum* cf.
168 *imlayi* Pessagno (Fig. 4, n° 3) and *Cinguloturris carpatica* Dumitrica (Fig. 4, n° 4). This
169 assemblage is assigned to UAZ 8-11 of Middle Callovian to Early Tithonian age.
170
171 In summary:
172 1. Our chert pebbles range in age from Late Bajocian-Early Callovian (UAZ 5-7) to Middle
173 Oxfordian-Early Tithonian (UAZ 8-11).

174 2. The oldest pebble could be as old as Late Bajocian (base of UAZ 5) but also as young as
175 Early Callovian (top of UAZ 7).
176 3. The youngest pebble could be as old as Middle Oxfordian (7057-14) and as young as Early
177 Tithonian (7057-14 or 7064-E1).
178 4. Three pebbles are Middle Jurassic in age. Among them, 7057-22 is restricted to UAZ 7 of
179 Late Bathonian-Early Callovian age. The two others 7057-3 and -15 are possibly of the same
180 age but could also be younger (UAZ 5-7 and UAZ 6-7 respectively).
181 5. Only one pebble (7057-14) is with certainty Late Jurassic in age. The three remaining
182 pebbles are either Middle or Late Jurassic (7057-8, 7057-20, and 7064-E1).

183

184

185 **4. Comparisons with previous radiolarian localities of the Piemont Schistes Lustrés zone**

186

187 4.1. Biochronology

188

189 As mentioned previously, only three localities of supraophiolitic radiolarites are dated so far
190 in the Schistes Lustrés complex of the French-Italian Alps. They range in age from Middle
191 Bathonian to Middle-Late Oxfordian:

192 1. the Cascavelier Peak radiolarite near Saint-Véran was originally dated as Late Oxfordian-
193 Middle Kimmeridgian (De Wever and Caby 1981). This age was later revised to the Middle
194 or Late Oxfordian (UAZ 9) (De Wever and Baumgartner 1995).

195 2. the Traversiera massif locality was originally found by R. Polino (Torino), with
196 radiolarians occurring in phosphate nodules at the base of the sedimentary cover of the
197 ophiolite (Y. Lagabrielle, pers. com. 2006). It was dated as Late Oxfordian-Early

198 Kimmeridgian (Schaaf et al. 1985), an age later revised as Late Bathonian-Early Callovian
199 (UAZ 7) (De Wever et al. 1987; De Wever et Baumgartner 1995).

200 3. the “Rocher de la Perdrix” radiolarites from the Chenaillet massif near Montgenèvre are
201 exposed in the Lago Nero-Replatte thrust sheet located structurally beneath the Chenaillet
202 ophiolite thrust sheet s.s.. It was tentatively assigned to UAZ 6 of Middle Bathonian age. It
203 could be the oldest radiolarite exposure of the Piemont zone (Cordey and Bailly 2007).

204

205 In comparing our results with these biochronological data, we find that the ages of
206 radiolarite pebbles overlap almost entirely the age range known from *in situ* Piemont Schistes
207 Lustrés radiolarite localities. Our results also lead to the following observations:

208 1. In our sampling, biozone UAZ 7 seems well represented in 2 pebbles, possibly 4. It
209 matches the age established in the Traversiera massif (Late Bathonian-Early Callovian).
210 2. The occurrence of biozone UAZ 6 known at the Chenaillet is not confirmed but could be
211 present in 2 of the 7 pebbles.

212 3. Our youngest pebble could be coeval to the Pic Cascavelier locality of Middle-Late
213 Oxfordian age (UAZ 9) but could also be younger (Kimmeridgian or Early Tithonian).

214

215 4.2. Faunal content

216

217 Some radiolarian morphotypes present in our pebbles were not reported before in the Piemont
218 Schistes Lustrés *in situ* radiolarites. The Pic Cascavelier locality (UAZ 7) has an assemblage
219 of sixteen species in which only *Homoeoparonaella argolidensis* Baumgartner occurs in one
220 pebble (7057-22). The St-Véran section (UAZ 9) comprises nineteen species in which only
221 *Acaeniotyle diaphorogona* Foreman and potentially *Bernoullius dicera* (Baumgartner) are
222 present in our assemblages. Finally, the Rocher de la Perdrix locality has only 5 morphotypes

223 with 2 species of the genus *Kilinora* which does not occur elsewhere. Overall, our pebbles
224 seem richer in nassellarians, including morphotypes of *Cinguloturris*, *Fultocapsa*,
225 *Protunuma*, *Pseudodictyomitrella*, *Pseudoristola*, *Pseudoeucyrtis*, *Stichocapsa*, *Yaocapsa* and
226 *Zhamoidellum* which were not reported in other localities of the Piemont Schistes Lustrés
227 zone (Bill et al. 2001). On one hand, these discrepancies may not be paleontologically
228 significant as they could result from taphonomical biases. On the other hand, they could
229 suggest that radiolarite beds stored as pebbles in molasse conglomerates have no *in situ*
230 equivalents, or that these equivalents have been entirely destroyed or metamorphosed. We
231 have presently no argument for preferring one of these hypotheses.

232

233

234 **5. Discussion and conclusions**

235

236 **5.1. The Alpine Tethys birth and spreading scenario**

237

238 The oldest radiolarite sample documented in our study is Late Bajocian or Early Callovian in
239 age. If we consider that *in situ* radiolarites of the Western Alps are associated with ophiolite
240 basements, this age remains compatible with the classical scenario of synchronous opening
241 for both the Central Atlantic and the Alpine Tethys in the Middle Jurassic (Lemoine et al.
242 2000, Bill et al. 2001, Cordey and Bailly 2007, de Graciansky et al. 2010). However we do
243 not know if the sampled molasses contain older oceanic remnants. In the outer Piemont zone,
244 the three thrust-sheets bearing diagnostic supraophiolitic radiolarites are imbricated with
245 thrust-sheets derived from the European distal margin (Caby et al. 1971, Tricart et al. 2003).
246 The simplest hypothesis is that our pebbles result from the erosion of ophiolite-bearing thrust-
247 sheets of a similar Piemont paleogeographic origin, i.e. the part of the ocean located at the

248 foot of the European margin. However, one cannot rule out a source in one or several now
249 entirely eroded units that originated from the other side of the ocean at the foot of the African
250 margin (Adria).

251

252 With the contribution of these fossiliferous pebbles, the number of radiolarites dated
253 so far in the Piemont zone of the Western Alps increases from 3 to 10. If the occurrence of
254 Kimmeridgian or Tithonian cherts was confirmed by future sampling, it would extend the
255 time span represented in these deep-sea sediments from 16 to 20 Myr. For an ocean with a
256 very low spreading rate of ~2 cm/year as expected for the Alpine Tethys (Lagabrielle and
257 Cannat 1990, Lagabrielle and Lemoine 1997, Lagabrielle 2009, Manatschal and Müntener
258 2009), this time span could correspond to 400 km in width. Of course this estimate is to be
259 considered with caution, as pebbles could come from any level of an original radiolarite
260 succession resting on a slightly older crust.

261

262 We do not bring any evidence for the occurrence of radiolarite sedimentation in the
263 Early Cretaceous and consequently an even wider oceanic domain. However most Tethyan
264 basin facies grade into pelagic limestones or shale/limestone alternation in the Late Tithonian
265 (Bill et al. 2001). All direct and indirect fossiliferous elements of the ocean found in ophiolite
266 covers and molasses are from the oldest parts of this domain, corresponding to remnants of
267 the so-called “narrow ocean” stage. As already observed elsewhere in the Alpine-Apennine
268 domain, radiolarite units are Middle and Late Jurassic without any evidence of Cretaceous
269 chert sedimentation (Bill et al. 2001). Apart from the Balma and Chiavenna units in the Valais
270 oceanic domain (93 Ma U/Pb ages; Liati and Froitzheim 2006), all other radiometric ages
271 overlap the age of radiolarian cherts (Manatschal and Müntener 2009). In the hypothesis of
272 ongoing Cretaceous rifting, elements of a younger and more axial part of this ocean remain to

273 be identified. If such elements are no longer exposed, they could remain hidden at depth.
274 They could also have been eroded after exhumation. If this is the case, further
275 investigation on foreland detrital formations is needed. However, the most probable
276 explanation is that during the Cretaceous, the Alpine Tethyan ocean was no more active and
277 the oceanic spreading was mostly accommodated in the Central Atlantic to the west and the
278 Neotethys to the east.

279

280 5.2. The Alpine orogenic wedge building scenario

281

282 During Early Oligocene times, the present-day Alpine internal zones inherited part of the
283 Eocene subduction-related accretionary wedge that had just undergone syncollisional
284 polyphase shortening (Tricart et al. 2006, Morag et al. 2008, Bernet and Tricart 2011). The
285 erosion of the new-born mountain range with exposed margin- and ocean-derived thrust
286 sheets fed rather abruptly the foreland molasses which show a great variety of lithologies, not
287 only radiolarites but also magmatic pebbles such as basalts and gabbros with greenschist to
288 blueschist facies, as well as serpentized peridotites with blueschist to eclogite facies (de
289 Gracianski et al. 1971, Schwartz et al., in press). As this foreland was progressively affected
290 by folding and forethrusting, Oligocene molasse basins born along the Alpine front evolved as
291 transported basins before being closed and incorporated to the Alpine wedge (present-day
292 external zone : see review in Ford et al. 2006).

293

294 Although *in situ* fossiliferous radiolarian cherts of the outer Piemont zone underwent
295 high greenschist or blueschist facies metamorphism, our study shows that some eroded
296 radiolarite units buried as molasse pebbles experienced low P-T conditions. This is supported
297 by the following observations: 1/ low silica recrystallization of pebbles's radiolarite matrices,

298 2/ absence of phengites in the pebbles microfacies; these white micas are commonly observed
299 in the HP blueschist siliceous facies of the Piemont zone, 3/ fair preservation of radiolarian
300 microfossils. It is also noteworthy that Mesozoic radiolarite pebbles of the Subalpine molasse
301 display much higher rates of microfossil recovery than *in situ* Mesozoic radiolarites of the
302 Piemont zone. Interestingly, the same low-grade metamorphism characterizes the chert
303 pebbles extracted from synorogenic conglomerates derived from the Mesozoic accretionary
304 complexes of western North America (Seiders and Blome 1984; Cordey, 1992a, b, Cordey
305 1998). There, some radiolarite pebbles have revealed the existence of ocean units whose
306 equivalent correlatives have never been found *in situ* (Cordey 1998). Our study suggests that
307 it is also the case in the Alps.

308

309 The occurrence of low-grade radiolarite pebbles indicate that some eroded thrust-
310 sheets originating from the oldest parts of the ocean escaped any serious tectonic burial during
311 the Alpine convergence (Fig. 5). The 20 Myr potential age range represented by our
312 radiolarite pebbles does not favor a single source. However, we do not know if these
313 radiolarites derived from the European side or from both sides of the ocean spreading-ridge.
314 Yet they show that by 30 Ma, the Alpine wedge had probably sampled the entire oceanic
315 sediments accreted at very contrasted structural levels in the accretionary wedge. The question
316 whether there is a link between the paleogeographic European or African origin of these
317 remnants and their structural history remains open. Future models for the building of the
318 Alpine wedge during early convergence will have to test the processes of a selective tectonic
319 sampling of these paleogeographic realms during accretion.

320

321

322 **Acknowledgements**

323 We thank Pierre-Charles de Graciansky (Paris) and Peter O. Baumgartner (Lausanne) for their
324 thorough and insightful reviews. This work was supported by the CNRS-UMR 5276 and the
325 ANR program “ERD-Alps” (Erosion and Relief Development in the western Alps). Chert
326 pebbles were processed in the radiolarian extraction laboratory of Université Lyon 1 (CNRS-
327 UMR 5276). We also thank Arlette Armand (Lyon) for SEM assistance.

328

329 **References**

330 Artoni, A., and Meckel, L., D., III (1998). History and deformation rates of a thrust sheet top
331 basin: the Barrême basin, western Alps, SE France. *Geological Society Special Publication*,
332 134, p. 213-237.

333

334 Barféty, J. C., Lemoine, M., Graciansky, P. C. de, Tricart, P., and Mercier, D. (1995). Notice
335 explicative, Carte géol. France (1/50 000), feuille Briançon (823), Orléans. *Bureau de*
336 *Recherches Géologiques et Minières*, 180 p.. Geological map by J.C. Barféty, M. Lemoine, D.
337 Mercier, R. Polino, P. Nievergelt, J. Bertrand, T. Dumont, S. Amaudric du Chaffaut, A.
338 Pêcher, G. Montjuvent.

339

340 Baumgartner, P.O., Bartolini, A., Carter, E.S., Conti, M., Cortese, G., Danelian, T., De
341 Wever, P., Dumitrica, P., Dumitrica-Jud, R., Gorican, S., Guex, J., Hull, D.M., Kito, N.,
342 Marcucci, M., Matsuoka, A., Murchey, B., O'Dogherty, L., Savary, J., Vishnevskaya, V.,
343 Widz, D., Yao, A. (1995). Middle Jurassic to Early Cretaceous radiolarian biochronology of
344 Tethys based on unitary associations, in: Baumgartner, P.O., *et al.* (Eds.), Middle Jurassic to

- 345 Lower Cretaceous Radiolaria of Tethys: Occurrences, systematics, biochronology. *Mémoires*
346 *de Géologie*, 23, Lausanne, 1013-1043.
- 347
- 348 Bernet, M., and Tricart, P. (2011). The Oligocene orogenic pulse in the Southern Penninic
349 Arc (Western Alps): structural, sedimentary and thermochronological constraints. *Bulletin de*
350 *la Société Géologique de France*, 182, 25-36. doi: 10.2113/gssgbull.182.1.25.
- 351
- 352 Bernoulli, D., and Jenkyns, H. (2009). Ancient oceans and continental margins of the Alpine -
353 Mediterranean Tethys: deciphering clues from Mesozoic pelagic sediments and ophiolites.
354 *Sedimentology*, 56, 149-190.
- 355
- 356 Bill, M., O'Dogherty, L., Guex, J., Baumgartner, P.O., and Masson, H. (2001). Radiolarite
357 ages in Alpine-Mediterranean ophiolites. Constraints on the oceanic spreading and the
358 Tethys-Atlantic connection. *Geological Society of America Bulletin*, 113, 129–43.
- 359
- 360 Bousquet, R., Oberhänsli, R., Goffé, B., Wiederkehr, M., Koller, F., Schmid, S. M., Schuster,
361 R., Engi, M., Berger, A., and Martinotti, G. (2008). Metamorphism of metasediments at the
362 scale of an orogen: a key to the Tertiary geodynamic evolution of the Alps. In Siegesmund,
363 S., Fügenschuh, B., and Froitzheim, N. (Eds.), *Tectonic Aspects of the Alpine-Dinaride-*
364 *Carpathian System* (pp. 393-411). The Geological Society of London.
- 365
- 366 Boussac, J. (1912). *Etudes statigraphiques sur le Nummulitique alpin*. Mémoire explicatif de
367 la carte géologique détaillée de la France, 662 pp.
- 368

- 369 Caby, R., Michard, A., and Tricart, P. (1971). Découverte d'une brèche polygénique à
370 éléments granitoïdes dans les ophiolites métamorphiques piémontaises (Schistes lustrés du
371 Queyras, Alpes françaises). *Comptes Rendus de l'Académie des Sciences Paris*, 273, sér. D,
372 999-1002.
- 373
- 374 Chauveau, J. C., and Lemoine, M. (1961). Contribution à l'étude géologique du synclinal
375 tertiaire de Barrême (moitié nord). *Bulletin de la Carte géologique de France*, 264, 147-178.
- 376
- 377 Cordey, F. (1992a). Radiolarians and Terrane Analysis in the Canadian Cordillera: the "clastic
378 approach". In Aitchison, J., and Murchey, B. (Eds.), The significance and application of
379 Radiolaria to Terrane Analysis. *Palaeogeography Palaeoclimatology Palaeoecology*, 96, 155-
380 159.
- 381
- 382 Cordey, F. (1992b). Radiolarian ages from chert pebbles of the Tantalus Formation, Carmacks
383 area, Yukon Territory. *Geological Survey of Canada Paper* 92-1E, 53-59.
- 384
- 385 Cordey, F. (1998). *Radiolaires des complexes d'accrétion cordillériens* (210 pp.). Geological
386 Survey of Canada Bulletin 509.
- 387
- 388 Cordey, F., and Bailly, A. (2007). Alpine ocean seafloor spreading and onset of pelagic
389 sedimentation: new radiolarian data from the Chenaillet-Montgenèvre ophiolite (French-
390 Italian Alps). *Geodinamica Acta*, 20, 131-138.
- 391

- 392 De Wever, P., and Caby, R. (1981). Datation de la base des Schistes lustrés postophiolitiques
393 par des radiolaires (Oxfordien supérieur-Kimméridgien moyen) dans les Alpes Cottiennes
394 (Saint-Véran, France). *Comptes Rendus de l'Académie des Sciences Paris*, 292, 467-472.
395
- 396 De Wever, P., and Baumgartner, P.O. (1995). Radiolarians from the base of the supra-
397 ophiolitic Schistes Lustrés Formation in the Alps (Saint-Véran, France and Traversiera
398 Massif, Italy). In Baumgartner, P.O., *et al.* (Eds.), Middle Jurassic to Lower Cretaceous
399 Radiolaria of Tethys: occurrences, systematics, biochronology. *Mémoires de Géologie*, 23,
400 Lausanne, 725-730.
- 401
- 402 De Wever, P., Danelian, T., Durand-Delga, M., Cordey, F., and Kito, N. (1987). Datations des
403 radiolarites post-ophiolitiques de Corse alpine à l'aide des Radiolaires. *Comptes Rendus de*
404 *l'Académie des Sciences Paris*, 305, 893-900.
- 405
- 406 Evans, M. J., and Elliott, T. (1999). Evolution of a thrust-sheet-top basin: the Tertiary
407 Barrême basin, Alpes de Haute Provence, France. *Geological Society of America Bulletin*,
408 111, 1617-1643.
- 409
- 410 Ferry, S., Tremblay, S., Guiraud, M. and Cordey, F. (2005). Les molasses rouges paléogènes
411 du bassin subalpin français. Corrélations avec le bassin helvétique. ASF Association
412 Sédimentologie France, Octobre 2005 (abstract).
- 413
- 414 Ford, M., and Lickorish, W. H. (2004). Foreland basin evolution around the western Alpine
415 arc. In Joseph, P., and Lomas, S. (Eds.). *Geological Society Special Publication*, 39-63.
- 416

- 417 Ford, M., Lickorish, W. H., and Kusznir, N. J. (1999). Tertiary foreland sedimentation in the
418 Southern Subalpine Chains, SE France: A geodynamic appraisal. *Basin Research*, 11, 315-
419 336.
- 420
- 421 Ford, M., Duchene, S., Gasquet, D., and Vanderhaeghe, O. (2006). Two-phase orogenic
422 convergence in the external and internal SW Alps. *Journal of the Geological Society*, 163, p.
423 815-826.
- 424
- 425 Gidon, M. (1971). Gap, Geological Map of France 1:50 000. *Bureau de Recherches
426 Géologiques et Minières*.
- 427
- 428 Gidon, M., Kerckhove, C., Michard, A., Tricart, P., Gotteland, P., Gout, C., Leblanc, D.,
429 Lefevre, R., Le Guernic, J., Mégard-Galli, J., and Michel-Noël, G. (1994). Aiguille de
430 Chambeyron, Geological Map of France 1:50 000. *Bureau de Recherches Géologiques et
431 Minières*.
- 432
- 433 Graciansky, P. C. de (1972). Le bassin tertiaire de Barrême (Alpes de Haute-Provence):
434 relations entre déformation et sédimentation; chronologie des plissements. *Comptes Rendus
435 de l'Académie des Sciences*, Paris, 275, 2825-2828.
- 436
- 437 Graciansky, P. C. de, Lemoine, M., and Saliot, P. (1971). Remarques sur la présence de
438 minéraux et de paragénèses du métamorphisme alpin dans les galets des conglomérats
439 oligocènes du synclinal de Barrême (Alpes de Haute-Provence). *Comptes Rendus de
440 l'Académie des Sciences*, Paris, 272, 3243-3245.
- 441

- 442 Graciansky, P. C. de, Roberts, D. and Tricart, P. (2010). *The Western Alps from rift to passive*
443 *margin to orogenic belt : an integrated geosciences overview* (432 pp.). Elsevier.
- 444
- 445 Gubler, Y. (1958). Etude critique des sources du matériel constituant certaines séries dans le
446 Tertiaire des Alpes françaises du Sud: formations détritiques de Barrême, Flysch "Grés
447 d'Annot". *Eclogae Geologicae Helvetiae*, 51, 942-977.
- 448
- 449 Lagabrielle, Y. (2009). Mantle exhumation and lithospheric spreading: an historical
450 perspective from investigations in the oceans and in the Alps-Appennines ophiolites. *Italian*
451 *Journal of Geosciences*, 128, 279-293.
- 452
- 453 Lagabrielle, Y. and Cannat, M. (1990). Alpine Jurassic ophiolites resemble the modern central
454 Atlantic basement. *Geology*, 18, 319-22.
- 455
- 456 Lagabrielle, Y. and Lemoine, M. (1997). Alpine, Corsican and Apennine ophiolites: the slow-
457 spreading ridge model. *Comptes Rendus de l'Académie des Sciences*, Paris, 325, sér. II, 909-
458 20.
- 459
- 460 Lemoine, M. (1983). Rifting and early drifting: Mesozoic Central Atlantic and Ligurian
461 Tethys. *Initial reports Deep Sea Drilling Project*, US Government Printing Office,
462 Washington DC, 76, 885-895.
- 463
- 464 Lemoine, M., and Tricart, P. (1986). Les Schistes lustrés piémontais des Alpes occidentales:
465 approche stratigraphique, structurale et sédimentologique. *Eclogae Geologicae Helvetiae*, 79,
466 271-94.

467

468 Lemoine, M., Steen, D., and Vuagnat, M. (1970). Sur le problème stratigraphique des
469 ophiolites piémontaises et des roches sédimentaires associées: observations dans le massif de
470 Chabrière en Haute-Ubaye (Basses-Alpes, France). *Archives des Sciences*, Genève, 5, 44-59.

471

472 Lemoine, M., Bas, T., Arnaud-Vanneau, A., Arnaud, A., Dumont, T., Gidon, M., Bourbon,
473 M., Graciansky, P.-C. d., Rudkiewicz, J.-L., Mégard-Galli, J., and Tricart, P. (1986). The
474 continental margin of the Mesozoic Tethys in the Western Alps. *Marine and Petroleum
475 Geology*, 3, 179-199.

476

477 Lemoine, M., Graciansky, P.-C. de, and Tricart, P. (2000). *De l'océan à la chaîne de
478 montagnes: tectonique des plaques dans les Alpes* (207 p.). Paris : Gordon and Breach
479 Science.

480

481 Liati, A., and Froitzheim, N. (2006). Assessing the Valais ocean, Western Alps: U-Pb
482 SHRIMP zircon geochronology of eclogite in the Balma unit, on top of the Monte Rosa
483 nappe. *European Journal of Mineralogy*, 18, 299-308.

484

485 Manatschal, G., and Müntener, O., (2009). A type sequence across an ancient magma-poor
486 ocean-continent transition: the example of the western Alpine Tethys ophiolites.
487 *Tectonophysics*, 437, 4-19.

488

489 Meckel, L., D., III, Ford, M., and Bernoulli, D. (1996). Tectonic and sedimentary evolution of
490 the Dévoluy Basin, a remnant of the Tertiary western Alpine foreland basin, SE France.
491 *Géologie de la France*, 2, 3-26.

492

493 Mevel, C., Caby, R., Kienast, J.-R. (1978). Lower amphibolite facies conditions in the oceanic
494 cruts: example of amphibolitized falser-gabbro and amphibolites from an alpine ophiolitic
495 massif (Chenaillet massif, Hautes Alpes, France). *Earth and Planetary Science Letters*, 39,
496 98-108.

497

498 Morag, N., Avigad, D., Harlavan, Y., McWilliams, O., and Michard, A. (2008). Rapid
499 exhumation and mountain building in the Western Alps: Petrology and $^{40}\text{Ar}/^{39}\text{Ar}$
500 geochronology of detritus from Tertiary basins of southeasern France. *Tectonics*, 27,
501 doi:10.1029/2007TC002142.

502

503 O'Dogherty, L., Bill, M., Gorican, S., Dumitrica, P., and Masson, H. (2006). Bathonian
504 radiolarians from an ophiolitic mélange of the Alpine Tethys (Gets Nappe, Swiss-French
505 Alps). *Micropaleontology*, 51, n° 6, 425-485.

506

507 Rüst, D. (1885). Beiträge zur Kenntniss der fossilen Radiolarien aus Gesteinen des Jura und
508 der Kreide. *Palaeontographica*, 31, 269-321.

509

510 Schaaf, A., Polino, R. and Lagabrielle, Y. (1985). Nouvelle découverte de radiolaires d'âge
511 Oxfordien supérieur-Kimméridgien inférieur à la base d'une série supra-ophiolitique des
512 schistes lustrés piémontais (Massif de Traversiera, Haut Val Maïra, Italie). *Comptes Rendus
513 de l'Académie des Sciences*, Paris, sér. II, 14, 1079-1084.

514

515 Schmid, S. M., Fügenschuh, B., Kissling, E., and Schuster, R. (2004). Tectonic map and
516 overall architecture of the Alpine orogen. *Eclogae Geologicae Helvetiae*, 97, 93-117.

517

518 Schwartz, S., Tricart, P., Guillot, S., Bernet, M., Chamorro-Perrez, E. M., Montagnac, G., and
519 Jourdan, S., *in press*. Source tracing of detrital serpentinite in the Oligocene molasse deposits
520 from the western Alps (Barrême basin): implications for relief formation in the internal zone.
521 *Geological Magazine*.

522

523 Seiders, V.M., and Blome, C.D. (1984). Clast compositions of Upper Mesozoic
524 conglomerates of the California Coast Ranges and their tectonic significance. In M.C. Blake
525 Jr. (ed.), *Franciscan Geology of Northern California* (pp. 135-148). Pacific Section of
526 Economic Paleontologists and Mineralogists 43.

527

528 Sissingh, W. (2001). Tectonostratigraphy of the West Alpine Foreland: correlation of Tertiary
529 sedimentary sequences, changes in eustatic sea-level and stress regimes. *Tectonophysics*, 333,
530 361-400.

531

532 Tricart, P. (1984). From passive margin to continental collision: a tectonic scenario for the
533 Western Alps. *American Journal of Science*, 284, 97-120.

534

535 Tricart, P., Amaudric du Chaffaut, S., Ayoub, C., Ballèvre, M., Caby, R., Gout, C.,
536 Lagabrielle, Y., Leblanc, D., Le Mer, O., Philippot, P., and Saby, P. (2003). Aiguilles-Col
537 Saint Martin Geological Map of France 1:50 000. *Bureau de Recherches Géologiques et*
538 *Minières*.

539

540 Tricart, P., Lardeaux, J.-M., Schwartz, S., and Sue, C. (2006). The late extension in the inner
541 western Alps: a synthesis along the south-Pelvoux transect. *Bulletin de la Société Géologique*
542 *de France*, 177, 299-310.

543

544 **Table and figures captions**

545

546 **Table 1.** Radiolarian contents of pebbles, biozones (UAZ) and ages (Baumgartner et al. 1995,

547 O'Dogherty et al. 2006). When available, UAZ range of each taxon is provided.

548

549 **Fig. 1.** Location map of southern French-Italian Alps (modified from Schmid et al. 2004).

550 Location of sampled molasse conglomerates: M, Montmaur, B, Barrême. Known sites with

551 *in-situ* bedrock fossiliferous radiolarites: P, Rocher de la Perdrix (Chenaillet Massif), C,

552 Cascavelier Peak (southern Queyras), T, Traversiera Massif. In red: major fault zones.

553

554 **Fig. 2.** Schematic stratigraphy of the Tertiary foreland series exposed in the French Subalpine

555 zones, more specifically the Barrême basin. Barton. = Bartonian, Priabon. = Priabonian,

556 Aquitan. = Aquitanian, congro. = conglomerate; biostr. = biostrome. The origin of Barrême

557 basin pebbles are the Clumanc conglomerates.

558

559 **Fig. 3.** Outcrop of “Nagelfluh” molasse conglomerate near the village of Montmaur; circles:

560 pebbles of red radiolarites.

561

562 **Fig. 4.** Middle and Late Jurassic radiolarians from Oligocene molasses chert pebbles

563 (Scanning Electron Microscope). For each microfossil: taxon, sample number, FC database

564 picture number, length of scale bar.

565 1- *Pseudoeucyrtis* sp., 7057-14, n° 10, 260 µm.

566 2- *Archeospongoprunum elegans* Wu, 7057-22, n° 13, 150 µm.

567 3- *Archeospongoprunum* sp., 7057-E1, n° 2, 250 µm.

568 4- *Cinguloturris carpatica* Dumitrica, 7057-14, n° 11, 200 µm.

- 569 5- *Cinguloturris* sp., 7057-22, n° 6, 130 µm.
- 570 6- *Archeodictyomitra apiarum* (Rüst), 7057-14, n° 26, 200 µm.
- 571 7- *Archeodictyomitra* sp., 7057-14, n° 28, 150 µm.
- 572 8- *Archeodictyomitra* sp., 7057-22, n° 20, 125 µm.
- 573 9- *Archeodictyomitra* sp., 7057-14, n° 14, 150 µm.
- 574 10- ?*Parvingula mashitaensis* Mizutani, 7057-14, n° 4, 230 µm.
- 575 11- *Parahsuum carpathicum* Widz and De Wever, 7057-14, n° 15, 150 µm.
- 576 12- *Yaocapsa* sp., 7057-15, n° 4, 160 µm.
- 577 13- *Protunuma* sp., 7057-14, n° 22, 140 µm.
- 578 14- ?*Stichomitra* sp., 7057-08, n° 14, 150 µm.
- 579 15- *Pseudodictyomitrella* cf. *tuscanica* Chiari, Cortese and Marcucci, 7057-22, n° 12, 100
580 µm.
- 581 16- *Zhamoidellum* cf. *argandi* O'Dogherty, Gorican and Dumitrica, 7057-15, n° 16, 130 µm.
- 582 17- *Zhamoidellum ovum* Dumitrica, 7057-14, n° 19, 160 µm.
- 583 18- *Stichocapsa* aff. *robusta*, 7057-08, n° 6, 150 µm.
- 584 19- *Zhamoidellum* sp., 7057-14, n° 27, 185 µm.
- 585 20- *Pseudoristola tsunoensis* (Aita), 7057-22, n° 22, 110 µm.
- 586 21- *Arcanicapsa* cf. *leiostraca* (Foreman), 7057-22, n° 3, 140 µm.
- 587 22- *Zhamoidellum* cf. *calamin* O'Dogherty, Gorican and Dumitrica, 7057-15, n° 7, 120 µm.
- 588 23- *Williriedellum* sp. 1 (O'Dogherty et al. 2006), 7057-22, n° 9, 150 µm.
- 589 24- *Podobursa* cf. *spinosa* Ozvoldova, 7057-14, n° 5, 200 µm.
- 590 25- ?*Fultocapsa* sp., 7057-22, n° 23, 130 µm.
- 591 26- *Acaeniotyle diaphorogona* Foreman, 7057-14, n° 1, 200 µm.
- 592 27-*Emiluvia* cf. *chica* Foreman, 7057-22, n° 15, 200 µm.

593 28- *Homoeoparonaella argolidensis* Baumgartner, 7057-22, n° 1, 200 µm.

594 29- *Bernoullius* cf. *dicerca* (Baumgartner), 7057-20, n° 6, 150 µm.

595 30- *Tritrabs rhododactylus* Baumgartner, 7057-22, n° 18, 200 µm.

596 31- *Mirifusus* sp., 7057-14, n° 3, 250 µm.

597

598 **Fig. 5.** Crustal cross-section model proposing an evolution for the southern Western Alps
599 during the Early Oligocene. At that time, the Piemont thrust sheets already stacked in the
600 upper Cretaceous-Paleocene subduction accretionary wedge underwent severe syncollision
601 shortening. It resulted in a major orogenesis so that erosion fed abruptly the peripheral
602 molasses in margin-derived and ocean-derived clasts whose metamorphic signatures range
603 from non or very low-grade to high-grade blueschist facies (Lz: lizardite; Atg: antigorite).

	Radiolarite pebbles						
Radiolarian taxa	7057-3	7057-15	7057-22	7057-8	7057-20	7064-E1	7057-14
<i>Acaeniotyle diaphorogona</i> Foreman 4-22							X
<i>Arcanicapsa</i> cf. <i>leiostraca</i> (Foreman)			X				
<i>Archeodictyomitra apiarum</i> (Rüst) 8-22					X	X	X
<i>Archeodictyomitra</i> sp.			X				X
<i>Archeospongoprnum elegans</i> Wu 6-?			X				
<i>Archeospongoprnum</i> cf. <i>imlayi</i> Pessagno	X					X	
<i>Bernoullius</i> cf. <i>dicera</i> (Baumgartner) 3-10					X		
<i>Cinguloturris carpatica</i> Dumitrica 7-11		X	X	X		X	X
<i>Cinguloturris</i> sp.			X				
<i>Emiluvia ordinaria</i> Ozvoldova 9-11							X
<i>Emiluvia</i> cf. <i>chica</i> Foreman 3-18			X				
? <i>Fultocapsa</i> sp.			X				
<i>Homoeoparonaella argolidensis</i> Baumgartner 4-11			X				
<i>Mirifusus</i> sp.			X				X
<i>Orbiculiformella</i> sp.	X						
<i>Parahsuum carpathicum</i> Widz & De Wever 7-11							X
? <i>Parvingula mashitaensis</i> Mizutani 8-15							X
<i>Podobursa</i> cf. <i>spinosa</i> Ozvoldova 8-13							X
<i>Praeconocaryomma</i> sp.				X	X		
<i>Protunuma</i> sp.							X
<i>Pseudodictyomitrella</i> cf. <i>tuscanica</i> Chiari, Cortese & Marcucci		X					
<i>Pseudoristola tsunoensis</i> (Aita) 6-7			X				
<i>Pseudoeucyrtis</i> sp.							X
<i>Stichocapsa robusta</i> Matsuoka 5-7	X						
<i>Stichocapsa</i> aff. <i>robusta</i> Matsuoka				X			
<i>Stichocapsa</i> sp.	X				X		
? <i>Stichomitra</i> sp.				X			
<i>Tritrabs rhododactylus</i> Baumgartner 3-13			X				
<i>Williriedellum</i> sp. 1 (O'Dogherty et al. 2006)			X				
<i>Yaocapsa</i> sp. 5-6		X					
<i>Zhamoidellum ovum</i> Dumitrica 9-11							X
Zham. cf. <i>argandi</i> O'Dogherty, Gorican & Dumitrica 6-7	X						
Zham. cf. <i>calamin</i> O'Dogherty, Gorican & Dumitrica		X					
<i>Zhamoidellum</i> sp.							X
Unitary Association Zones UAZ	5-7	6-7	7	7-11	8-10	8-11	9-11
Age ranges	Late Baj. or Early Bath. to Early Call.	Mid. Bath. to Early Call.	Late Bath. to Early Call.	Late Bath. or Early Call. to Late Kim. or Early Tith.	Mid Call. to ? Early Kim.	Mid Call. to Late Kim. or Early Tith.	Mid Oxf. to Late Kim. or Early Tith.

Table 1

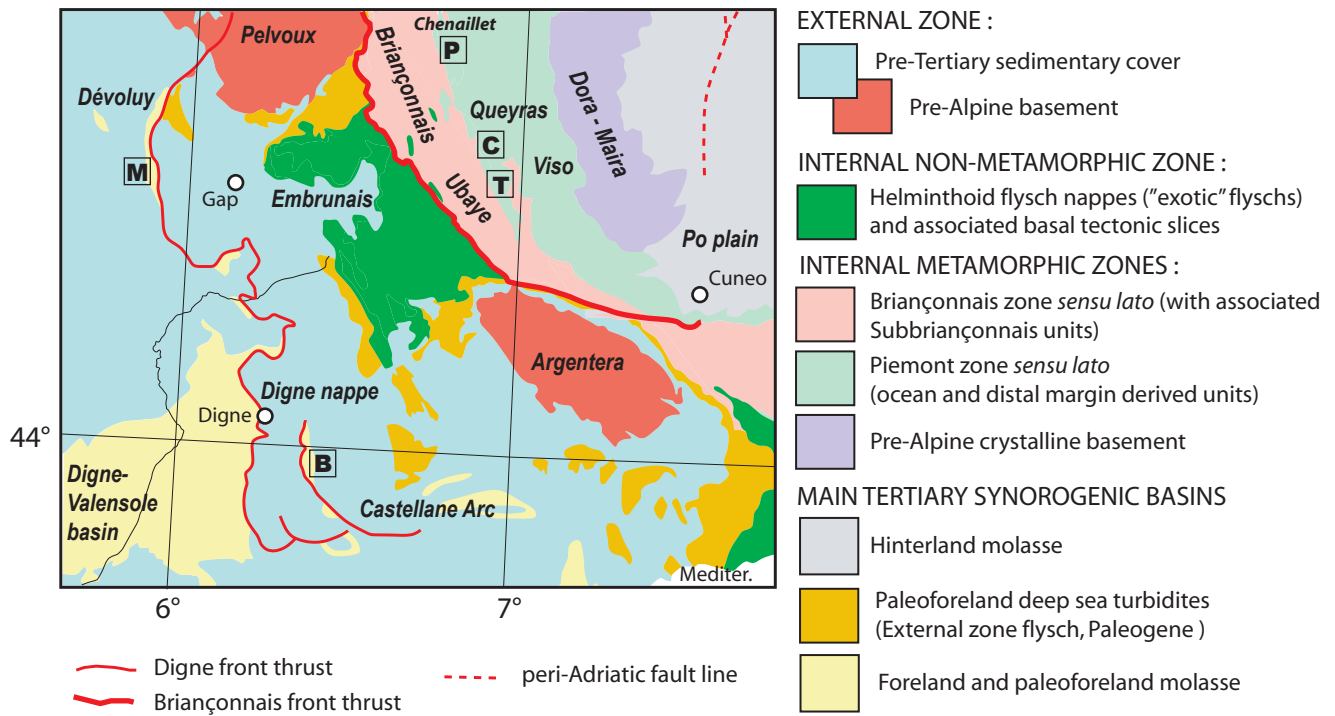


Fig. 1

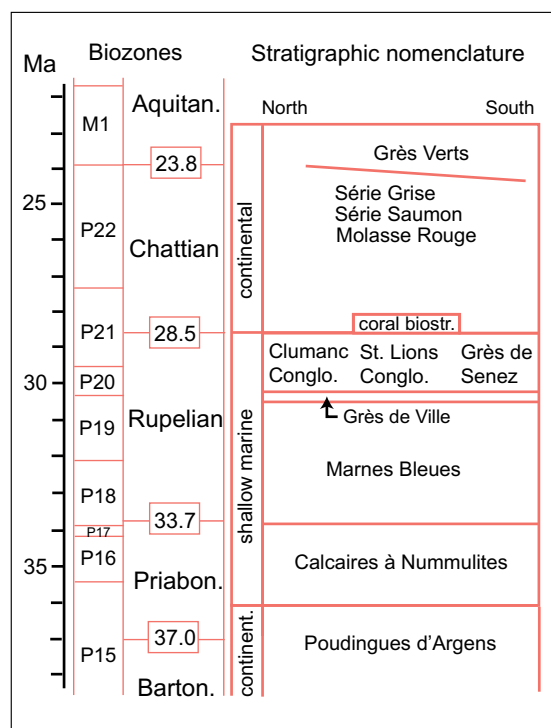


Fig. 2



Fig. 3

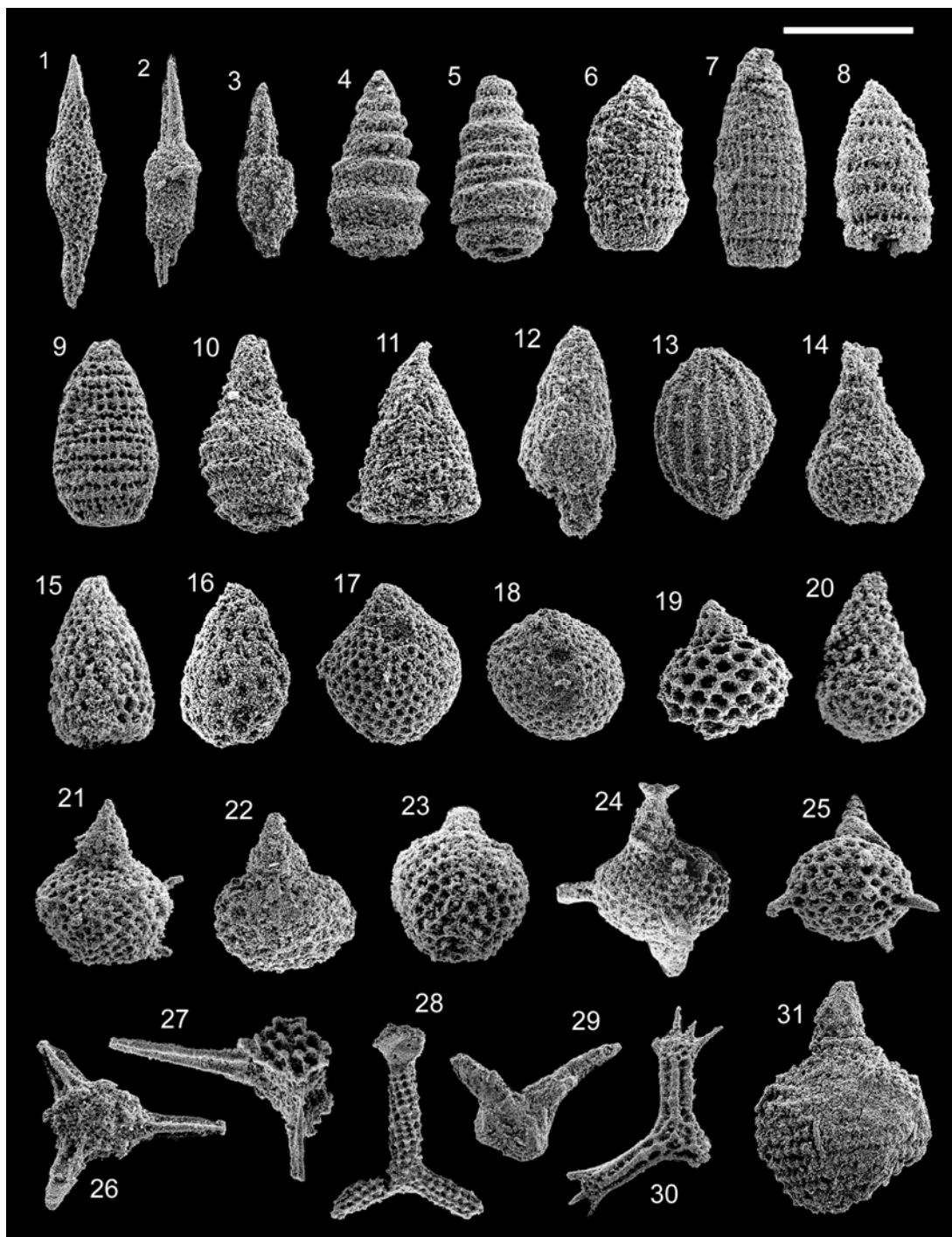


Fig. 4

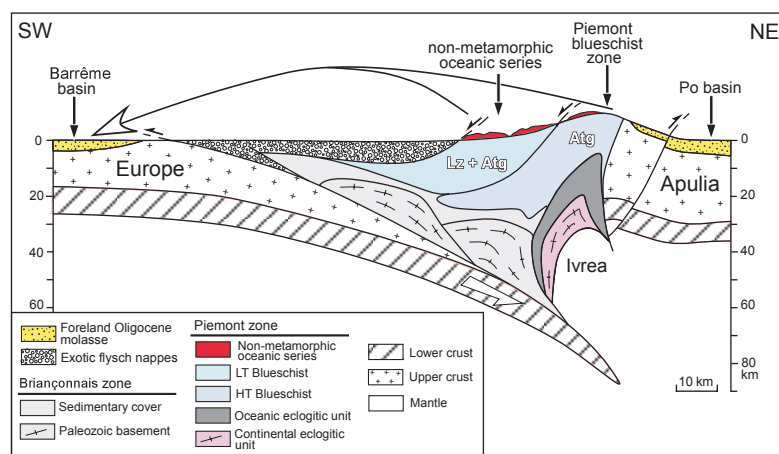


Fig. 5